

Effects of near-fault records characteristics on seismic performance of eccentrically braced frames

Reyhaneh Eskandari^a and Davoud Vafaei^{*}

Department of Civil Engineering, Chabahar Maritime University, Chabahar, Iran

(Received May 12, 2015, Revised October 13, 2015, Accepted November 16, 2015)

Abstract. In this paper the effects of fling-step and forward-directivity on the seismic performance of steel eccentrically braced frames (EBFs) are addressed. Four EBFs with various numbers of stories (4-, 8-, 12- and 15-story) were designed for an area with high seismic hazard. Fourteen near-fault ground motions including seven with forward-directivity and seven with fling-step effects are selected to carry out nonlinear time history (NTH) analyses of the frames. Furthermore, seven more far-field records were selected for comparison. Findings from the study reveal that the median maximum links rotation of the frames subjected to three set of ground motions are in acceptable range and the links completely satisfy the requirement stated in FEMA 356 for LS performance level. The arrival of the velocity pulse in a near-fault record causes few significant plastic deformations, while many reversed inelastic cycles result in low-cycle fatigue damage in far-fault records. Near-fault records in some cases are more destructive and the results of these records are so dispersed, especially the records having fling-step effects.

Keywords: seismic performance; eccentrically braced frame; near-fault earthquake; fling-step; forward-directivity

1. Introduction

Severe failures of modern-engineered structures observed within the proximity of active faults in many worldwide earthquakes have revealed that the effects of near-fault earthquakes on structures are significantly different from far-field ones. Though, there is no well-defined distance over which a site may be classified as in near or far-field, it is unlikely to exhibit the special effects of these earthquakes more than 10 to 15 km away from the rupture (Champion and Liel 2012, Iervolino and Cornell 2008). The main consequences of these earthquakes, which can impose unexpected seismic demands on structures, are fling-step and forward-directivity. Where the fault rupture propagates forward toward the site with a velocity close to the shear-wave velocity, and the direction of the fault slip is aligned with the site, forward-directivity occurs. This is accompanied by generating long-period, short-duration, and large-amplitude pulses in the velocity time histories (Somerville 1998). Fling-step related to the permanent tectonic deformations at the site. This is generally characterized by a unidirectional high velocity pulse with a uniform step in the

^{*}Corresponding author, Lecturer, E-mail: d.vafaei@cmu.ac.ir

^aLecturer., E-mail: r.eskandari@cmu.ac.ir

displacement time history (Kalkan and Kunnath 2006). Fling-step effect has been observed in limited near-fault ground motions such as in 1999 (Kocaeli 1999) Chi-Chi in Taiwan and 2011 Tohoku in Japan (Hamidi Jamnani *et al.* 2013). Further information about forward-directivity and fling-step can be found in Kalkan and Kunnath (2006).

There are many studies in the literature which investigated the effects of near-fault excitation on different types of structures. Most of these studies only considered the forward-directivity effect of these records, such as (Alavi and Krawinkler 2004, Dicleli and Mehta 2007, Gerami and Abdollahzadeh 2015, Gerami and Sivandi-Pour 2014, Huang *et al.* 2014, Malhotra 1999, Soleimani Amiri *et al.* 2013). In case of considering fling-step effects there are little reported works. In a study, three existing steel special moment resisting frames simulated to evaluate their seismic resistance under forward-directivity and fling-step near-fault ground motions. Their results compared to the response of buildings subjected to typical far-fault records. Additionally, idealized pulses utilized in a separate study to gain further insight into the effects of high-amplitude pulses on structural demands (Kalkan and Kunnath 2006).

In 2010, Mortezaei *et al.* studied the effect of fling-step near-fault records on the performance of fiber reinforced polymer (FRP) strengthened reinforced concrete buildings (Mortezaei *et al.* 2010). Moreover consequences of forward-directivity and fling-step on existing typical multi-span simply supported (MSSS) bridges were investigated with Ghodrati Amiri *et al.* (2011). The results of analyses showed that bridge structure stock to near-fault ground motions could be subjected to a large permanent displacement at the pier top of bridges at the arrival of the velocity pulse. Also the structural system was obliged to dissipate the input seismic energy in a single plastic cycle (Ghodrati Amiri *et al.* 2011).

In 2015 Vafaei and Eskandari, published their findings on 4-story, 8-story, 12-story and 15-story steel buckling-restrained braced frames (BRBFs) with mega configuration, subjected to near-source earthquakes. To seismic performance assessment of the BRBFs, fourteen near-fault records with forward-directivity and fling-step characteristics and seven far-faults had been used. Their study mentioned that near-fault records imposed higher demands on the structures. The results for near-fault records with fling-step were very dispersed, and in some cases, these records were more damaging than others (Vafaei and Eskandari 2015b). In another study the seismic performance of steel mega braced frames equipped with shape-memory alloy braces under near-fault earthquakes having forward-directivity and fling effects was assessed; and the results compared to the response of buildings to far-fault records (Vafaei and Eskandari 2015a).

From these studies it was determined that use of high ductility systems with ability of absorbing high amount of seismic input energy under near-fault records is unavoidable. Steel eccentrically-braced frame (EBF) is an effective load-resisting system for building structures to resist high wind and seismic loads. The main characteristic of an EBF is having high elastic stiffness of a conventional concentrically braced frame (CBF) while it can provide high levels of ductility similar to a well-detailed moment resisting frame (MRF). Bracing system supply the high elastic stiffness of EBFs, and the large ductility capacity is provided by transmitting the brace force to another brace or to a column through shear and bending in a beam segment which called link. In EBFs all inelastic activity is confined to this segment and other elements remain in elastic range (Tsai *et al.* 1993).

Although a huge body of knowledge exists on the steel eccentrically braced frames that are used for seismic resistance (Chao and Goel 2005, Engelhardt and Popov 1989, Gerami and Sivandi-Pour 2014, Ghobarah and Ramadan 1991, Kuşyılmaz and Topkaya 2013, 2015, Okazaki *et al.* 2006, Özhendekci and Özhendekci 2008, Rides and Popov 1994, Viswanath *et al.* 2010), but

there is a lack of information about the global performance of these kinds of structures in the proximity of an active fault. So, the objective of this study is to examine the response of EBFs to near-fault ground motions. To address this issue, four frames with different heights were designed for a high seismically active area. Near-fault ground motions were carefully selected so as to reflect the main characteristics of these records, i.e., forward-directivity and fling effects. These ground motions were used in nonlinear dynamic analyses, and their results were compared to the response of frames to typical far-fault records.

2. Design procedure

In this study a series of four-story, eight-story, 12-story and 15-story idealized EBF buildings were designed in accordance with three main specifications namely, Minimum Design Loads for Buildings and Other Structures (ASCE7-10) (ASCE7-10 2010), Seismic Provisions for Structural Steel Buildings (AISC 341-05) (AISC341-05 2005), and Specification for Structural Steel Buildings (AISC360-05) (AISC360-05 2005). Also the below mentioned design procedure was considered.

- 1) Determination of the design factors (R , C_d and Ω_0).
- 2) Determination of the design equivalent lateral force.
- 3) Selection of a link length.
- 4) Choosing an appropriate link section.
- 5) Design braces, columns and beam segments outside of the links
- 6) Control the maximum allowable interstory drift and plastic rotation of shear links.

It is noticeable that some of these steps iterated for several times to earn the best design.

Frames were assumed to be located in Los Angeles with $S_{DS}=1.353$ and $S_{D1}= 0.695$, where S_{DS} and S_{D1} are the site design spectral accelerations at 0.2 and 1.0 s in terms of gravity acceleration. The local site class was chosen as D . The dead and live (or snow) loads of 4 and 1.5 kN/m² were used in roof level and 4.7 and 2 kN/m², were used in second levels for gravity loads. Due to absence of at least two bays of seismic force-resisting perimeter framing on each side of the structure a redundancy factor of 1.3 was considered. The structures were assumed to be Risk Category II structures with an importance factor equal to unity. The following system design factors were used for EBFs: response modification coefficient, $R=8$; deflection amplification factor, $C_d=4$ and the system overstrength factor, $\Omega_0=2$.

To determine the member design forces, a two-dimensional analytical model of the prototype frame was constructed and an elastic analysis was performed. In each direction the lateral load was resisted by two braced bays with non-moment-resisting beam-column connections and the gravity framing was attached to the braced bay by making use of simple connections. A moment-resistant connection was assumed between braces and beams (Koboevic and David 2010), so that proper redistribution of the moment between the two elements could take place. Nominal yield strength equal to 350 MPa was used for all elements. As shown in Fig. 1, all designed frames have four 9 m-long bays and the story height of 3.8 m. The chevron-type configuration was preferred to avoid the beam-to-column connection in the link region. This kind of connections (link-to-column) are susceptible to fracture and in some cases are unable to achieve rotations beyond 0.07 rad (Okazaki *et al.* 2006).

Selection of the link length, e , is often restricted by architectural or other configuration restraints. In the present study due to absence of restraints, all EBF links were assumed 1 m in

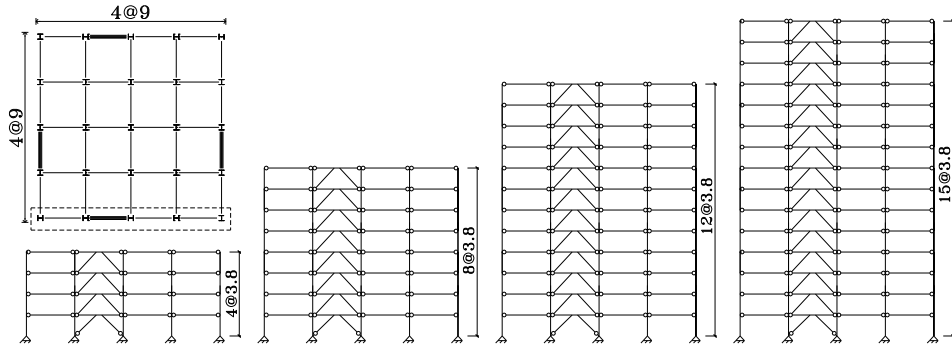


Fig. 1 Plane and brace configuration of the structures

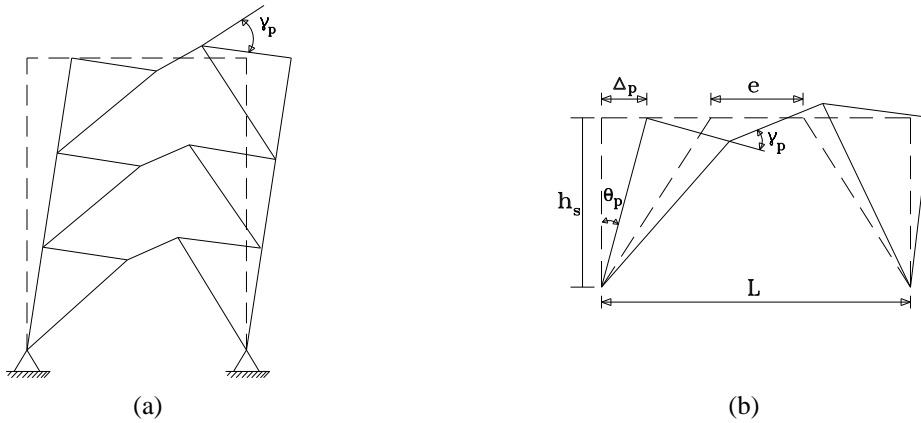


Fig. 2 (a) Typical deformation pattern of an EBF, (b) Rigid plastic mechanism

length. To avoid concentration of yielding in only a few stories, the strength-to-demand ratios of the links were selected as uniform as possible over the height of the frame (Popov *et al.* 1992). Since shear yielding of a link is the most ductile yielding mode (Daneshmand and Hosseini Hashemi 2012, Ghojarah and Ramadan 1991, Özhendekci and Özhendekci 2008, Richards and Uang 2005), the links sections designed to yield in shear (classified as short links). This was done by checking $e \leq 1.6M_p/V_p$ (Kasai and Popov 1986), where M_p and V_p are, respectively, nominal plastic flexural strength and nominal shear strength of the link.

According to AISC341-05 the maximum allowable inelastic shear rotation angle ($\gamma_{p-allowable}$) of short links is equal to 0.08 rad. γ_p , can be easily obtained from inelastic drift estimates considering a rigid-plastic mechanism (see Fig. 2 and Eq. (10)).

$$\begin{cases} \gamma_p = \frac{L}{e} \theta_p \\ \theta_p = \frac{\Delta_p}{h_s} \end{cases} \Rightarrow \gamma_p = \frac{L}{e} \frac{\Delta_p}{h_s} \quad (1)$$

where L =bay width, h_s =story height, Δ_p =plastic story drift which can be conservatively taken as

Table 1 Summary of member sizes for designed frames

Story	Column	beam	Brace	Story	column	beam	Brace
(a) four story				(b) eight story			
1	W14×82	W18×97	W12×120	1	W14×211	W16×100	W14×132
2	W14×68	W18×71	W14×159	2	W14×211	W16×100	W14×132
3	W14×48	W16×57	W14×159	3	W14×132	W16×89	W14×132
4	W14×48	W12×45	W12×45	4	W14×132	W16×89	W14×132
				5	W14×68	W14×82	W12×96
				6	W14×68	W14×74	W12×96
				7	W14×48	W14×48	W12×96
				8	W14×48	W8×40	W12×96
(c) twelve story				(d) fifteen story			
1	W14×398	W18×143	W14×159	1	W14×550	W21×147	W14×176
2	W14×342	W18×143	W14×159	2	W14×550	W21×147	W14×176
3	W14×342	W21×122	W14×159	3	W14×426	W18×158	W14×176
4	W14×283	W12×190	W14×159	4	W14×426	W18×158	W14×176
5	W14×211	W14×193	W14×159	5	W14×342	W18×158	W14×176
6	W14×193	W14×176	W14×159	6	W14×342	W18×158	W14×176
7	W14×159	W12×152	W12×120	7	W14×257	W18×158	W14×176
8	W14×159	W14×145	W12×120	8	W14×257	W18×143	W14×159
9	W14×132	W12×120	W12×120	9	W14×159	W18×119	W14×159
10	W14×82	W12×96	W12×120	10	W14×159	W18×119	W14×159
11	W14×48	W14×48	W12×120	11	W14×132	W18×106	W14×132
12	W14×48	W8×48	W12×120	12	W14×132	W16×89	W14×132
				13	W14×82	W14×82	W12×120
				14	W14×48	W14×53	W12×120
				15	W14×48	W8×48	W12×120

the design story drift (Δ). In addition, allowable story drift is given as $0.02 \times h_s$ for EBFs under Risk Category I and II in ASCE7-10.

The braces, columns and beams outside of links were designed for the maximum forces that generated by the links. Thus, these elements remain essentially elastic. Links, beams and braces were selected among American wide flange sections (W shapes), whereas columns were selected from W14 sections. The Links, columns and even the braces were designed to have seismically compact sections. More detailed description of design procedure can be found in Kuşyılmaz and Topkaya (Kuşyılmaz and Topkaya 2013, 2015). The final designed sections are summarized in Table 1.

3. Analytical model development

The Open Systems for Earthquake Engineering Simulation (OpenSees) Framework was used to model the 2D frames and perform nonlinear time history analyses (Mazzoni *et al.* 2007). Modeling

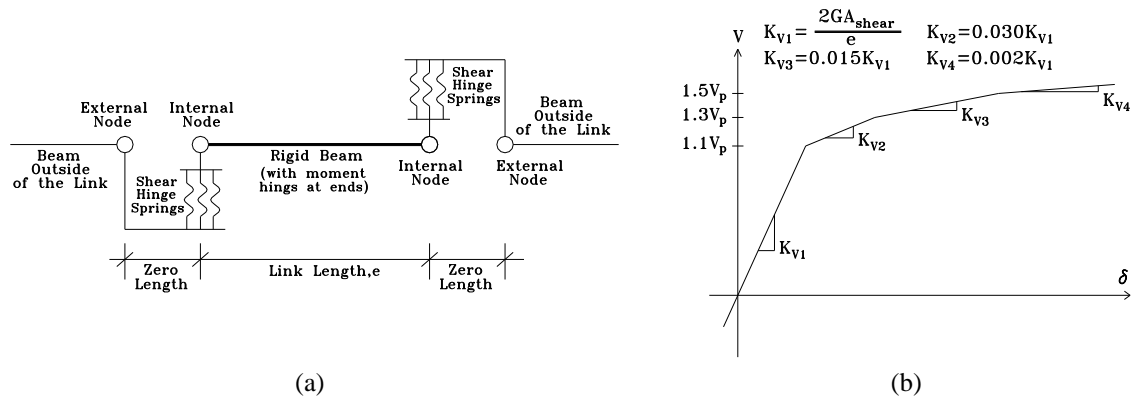


Fig. 3 (a) EBF link element, (b) combined behavior of parallel translational springs

Table 2 Modal periods of the EBFs

No. of stories	Periods (s)		
	1	2	3
4	0.626	0.246	0.147
8	1.380	0.484	0.269
12	2.025	0.645	0.343
15	2.596	0.798	0.413

of the braces, columns and beams outside of links with distributed plasticity were done by force-based nonlinear beam-column element with fiber sections. Since in the formulation of this element both usual and geometric stiffness matrix was contributed, it is capable of predicting linear or nonlinear buckling of elements during severe earthquakes (Uriz *et al.* 2008). To model steel's behavior, Steel02, a uniaxial steel material, which is a modified version of the well known Giuffre-Menegotto-Pinto model (Menegotto and Pinto 1973), was assigned to the elements. In case of simulation of the panel zones, since all beams were considered as pin-ended connections and the columns were designed to have a reasonable shear capacity, the panel zone yielding would not occur. Also expected elastic shear deformations were minimal. So the panel zones were not modeled explicitly.

EBFs shear links were modeled using the techniques proposed by Ghobarah and Ramadan (1991) (Ghobarah and Ramadan 1991) and modified slightly by Richards and Uang (2006) with a correlation study that compared the analytical and experimental results for some of the University of Texas, Austin (UTA) links with A992 steel (Richards and Uang 2006). Fig. 3(a) shows the link element used, consisting of a rigid beam element with lumped plasticity, and translational springs in series at each end. To model the rigid segment with lumped plasticity, beamWithHinges element was used and zero-length element modeled the translational springs in either end of the link. Three parallel translational springs, which combined behavior of them is shown in Fig. 3(b), tied the vertical deformation of the zero-length nodes. For horizontal and rotational deformations, equal degrees of freedom were considered.

One half of the total building mass was applied to the frames and the Newmark method with its commonly used values ($\gamma=0.5$ and $\beta=0.25$) was utilized to solve the equations of motions. In the

dynamic analysis, the 2% Rayleigh damping was specified in the first and third modes. Tangential stiffness matrix, which was suggested by Charney, was exclusively used to compute the damping matrix (Charney 2008). The adopted modal frequencies are listed in Table 2.

4. Selected ground motion records

Nonlinear time history analyses of the eccentrically braced frames were carried out by employing twenty one ground motion records. These records consist of three sets, (i) seven ordinary far-fault records, (ii) seven near-fault records characterized with forward-directivity effect and (iii) seven near-fault records characterized with fling-step displacements.

Table 3 Some characteristics of the utilized ground motions

No.	Year	Earthquake	M _w	Recording Station	Dist. ^a (km)	PGA ^b (g)	PGV ^c (cm/s)	Fling disp. (cm)
(a) Far-Fault Recordings								
1	1952	Kern county	7.5	Taft	36.2	0.18	17.5	—
2	1979	Imperial-Valley	6.5	Calexico		0.28	42.49	—
3	1989	Loma Prieta	7	Presidio	67.4	0.1	12.91	—
4	1971	San Fernando	6.6	Castaic, Old Ridge	23.5	0.17	25.9	—
5	1992	Big Bear	6.4	Desert Hot Spr.	40.1	0.23	19.14	—
6	1994	Northridge	6.7	Century CCC	23.7	0.25	21.19	—
7	1994	Northridge	6.7	Terminal Island	57.5	0.19	12.09	—
(b) Near-Fault Recordings (Forward-Rupture Directivity)								
1	1979	Imperial-Valley	6.5	El Centro	5.6	0.35	71.23	—
2	1999	Kocaeli	7.4	Duzce	11	0.31	58.85	—
3	1992	Cape Mendocino	7.1	Petrolia	15.9	0.66	90.16	—
4	1992	Erzincan	6.7	Erzincan	2	0.5	64.32	—
5	1994	Northridge	6.7	Rinaldi	8.6	0.84	174.79	—
6	1994	Northridge	6.7	Olive View	6.4	0.84	130.37	—
7	1987	Superstition Hills	6.4	Parachute Test Site	0.7	0.45	112	—
(c) Near-Fault Recordings (Fling-Step)								
1	1999	Kocaeli	7.4	Sakarya	3.2	0.41	82.05	186.76
2	1999	Kocaeli	7.4	Yarimca	3.3	0.23	88.83	145.97
3	1999	Chi-Chi	7.6	TCU052	1.8	0.44	216	697.12
4	1999	Chi-Chi	7.6	TCU068	3	0.5	277.56	601.84
5	1999	Chi-Chi	7.6	TCU074	13.8	0.59	68.9	174.56
6	1999	Chi-Chi	7.6	TCU071	4.9	0.63	79.11	181.64
7	1999	Chi-Chi	7.6	TCU079	11	0.57	68.06	153.05

^aClosest distance to fault rupture

^bPeak ground acceleration

^cPeak ground velocity

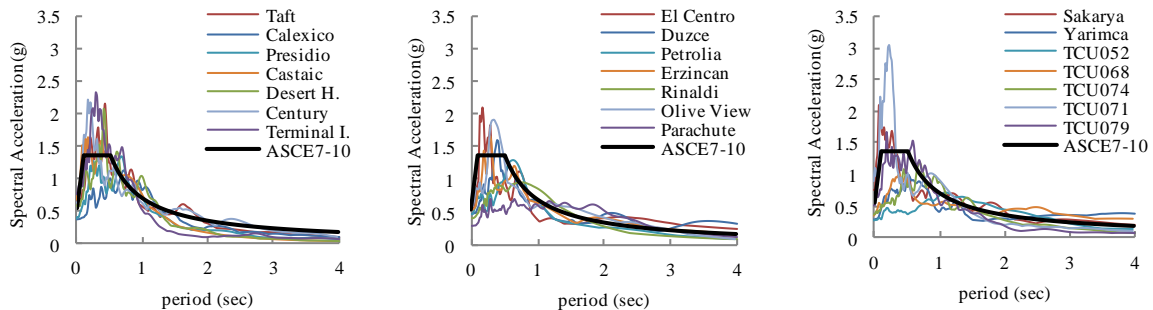


Fig. 4 Design spectrum and individual earthquake spectra (5% damping)

Ordinary far-fault ground motions contains records either taken from soil or stiff soil sites and recorded within 80 km of the causative fault plane from earthquakes having a magnitude (M_w) range of 6.4 to 7.5. Forward-directivity near-fault records were populated from the SAC steel project (Somerville *et al.* 1997b) and the California Division of Mines and Geology (CDMG) Strong Motion Instrumentation Program (Somerville 1998). These records are from earthquakes in the magnitude (M_w) range of 6.4 to 7.4 at soil or stiff soil sites and the maximum source-to-site distance of 15.9 km. The final set of ground motions (fling-step near-fault records) were recorded from the Kocaeli (1999) ($M_w=7.4$) and Chi-Chi 1999 ($M_w=7.6$) earthquakes at distances of 3.2 to 13.8 km. Further detailed information corresponding to the selection of the ground motions can be found in Kalkan and Kunnath (2006). Some characteristics of the utilized ground motions are listed in Table 3.

These ground motion were scaled in such a manner that the spectrum of each record matched the five percent damped ASCE7-10 design spectrum with minimum error in the period range of 0.6 sec to 4.0 sec. Fig. 4 shows the scaled acceleration spectra for the each set of earthquake records along with the design acceleration spectrum for the site.

5. Evaluation of seismic response characteristics

Nonlinear response-history (NRH) analyses were performed for 84 different cases to investigate the consequences of well-known characteristics of near-fault ground motions on the seismic response of four eccentrically braced frames. Inelastic link rotation (γ), defined as the inelastic angle between the link and the beam outside of the link, was used as the primary measure of seismic demand. The peak inelastic link rotation (γ_{max}) profiles obtained from NRH analyses of the EBFs are presented in Figs. 5 to 8 with their associated dispersion values. Also these figures indicate the maximum permissible plastic rotation values of the links for Immediate Occupancy (IO), Life Safety (LS), and Collapse prevention (CP) performance levels prescribed by FEMA 356. The basic criterion followed in the seismic performance evaluation of the ordinary structures, with an importance factor equal to unity, is LS performance; therefore this performance level is considered the upper bound of acceptable damage. Based on FEMA 356 for link beams that are controlled by shear (short links) the maximum permissible plastic rotation for IO, LS and CP performance levels are 0.005, 0.11 and 0.14 radians, respectively. Although the value of 0.11 rad for LS performance level is more than the AISC limitation of 0.08 rad, experimental testing by Okazaki *et al.* (2007) which was conducted at the University of Texas, Austin (UTA), revealed that

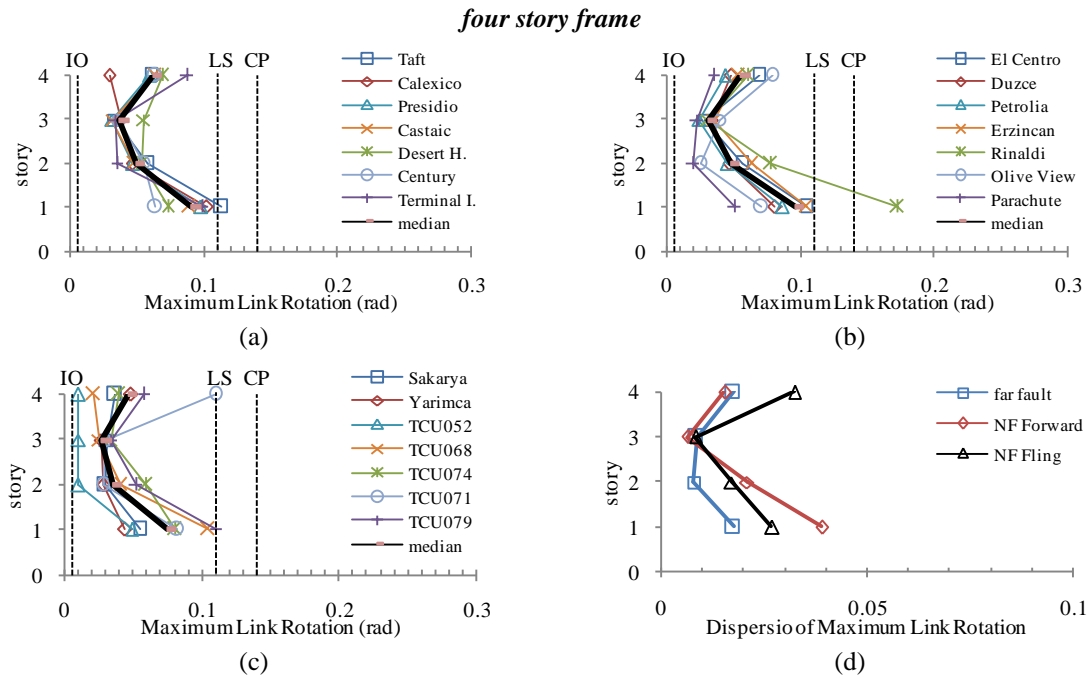


Fig. 5 Maximum link rotation of 4 story frame for (a) far-fault records, (b) near-fault records with forward directivity, (c) near-fault records with fling step, and (d) Dispersion of the results

shear yielding links under new AISC loading protocol are able to achieve inelastic rotations of 0.11 rad without stiffness and strength degradation (Okazaki and Engelhardt 2007). The new AISC loading protocol is believed to be more representative of demands caused by actual earthquake ground motion than the old-AISC protocol, on the basis of findings in Richards and Uang (2006) (Richards and Uang 2006).

For the 4 story frame, the maximum link rotation was concentrated at the first story for most records, with the exception of Olive-View and TCU071 records, which activation of higher-modes resulted in significant demand in upper story levels. The results of near-fault motions were more disperse and the lowest and highest link plastic rotation was occurred by these motions. Of the entire ground motions, the Rinaldi record with forward-directivity effects generated the highest link plastic deformation (0.17 rad which is even more than the maximum permissible plastic rotation for CP performance level) and TCU052 record with fling effects produced the lowest (0.009 rad). Comparison of the median profiles indicated that for three set of ground motions, γ_{ave} at each floor are well below the LS performance level limitation of 0.11 rad.

For the 8 story frame, the significant link deformation for most of the far-field records was shown to be either at the first or eighth floors. Although similar observations hold for near-fault earthquakes with forward-directivity, the demands at the intermediate levels were much higher. In the case of near-fault records with fling effects, due to different frequency content of the motions, the maximum demand did not concentrated at a specific story level. Also for most of these records nearly uniform distribution of inelastic response over the height of the buildings were shown. The maximum demand of three sets of ground motions, which caused by Desert H., Parachute and Sakarya records, was 0.18, 0.165 and 0.216 rad, respectively. Though these values of rotations are

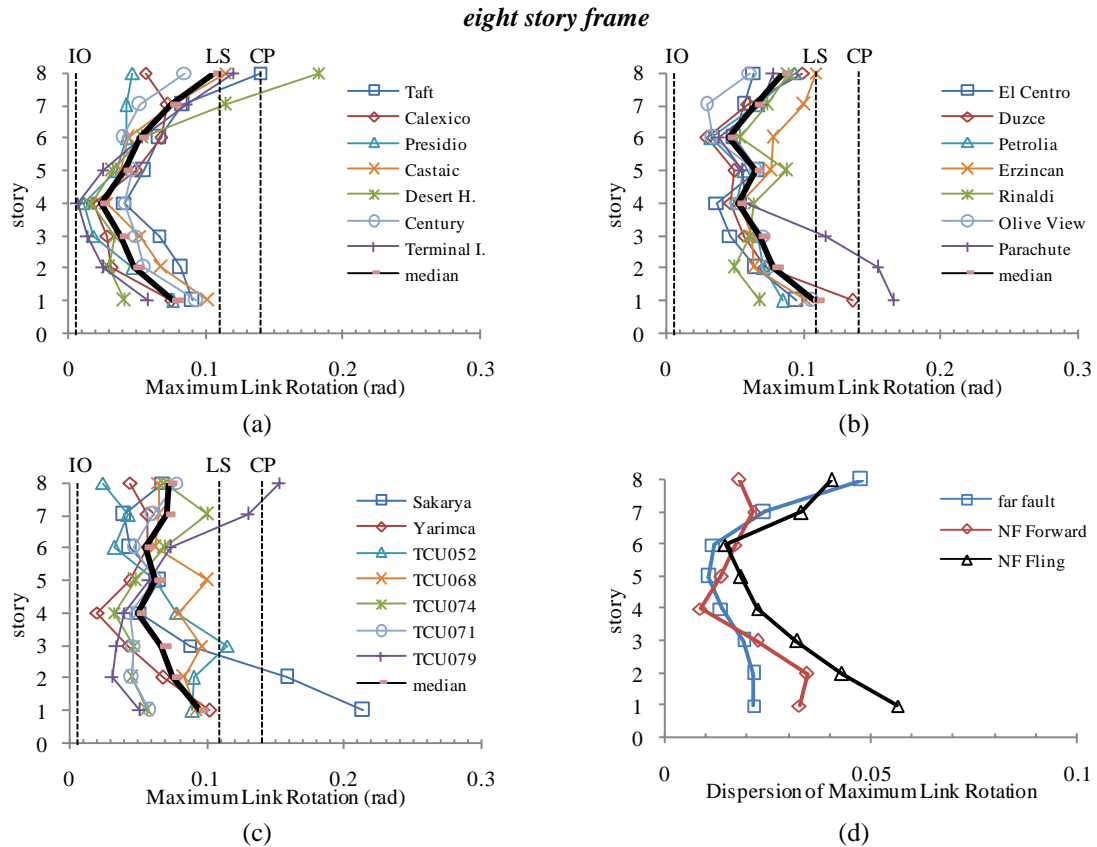


Fig. 6 Maximum link rotation of 8 story frame for (a) far-fault records, (b) near-fault records with forward directivity, (c) near-fault records with fling step, and (d) Dispersion of the results

much more than LS performance limitation, peak of the median link deformation for three sets of ground motions (0.106, 0.0108 and 0.095 rad, respectively for far-fault records, near-fault records with forward-directivity and near-fault records with fling-step) are below the upper bound of acceptable damage (0.11 rad). For the 8 story frames, the maximum dispersion of the results showed by the near-fault records with fling-step.

For the 12 and 15 story frames, the similar profiles were observed for all the far-fault records and triggering higher-mode effects resulted in increased demands in upper story levels. For the majority of near-fault ground motions the similar results were observed and the maximum link inelastic rotation was shown in the upper stories, but more effects of the first mode for several records like El Centro, Yarimca and Sakarya caused a shift in demands from upper stories to first floor. The significant dispersion of the results was shown for near-fault records, especially by fling effects. These records imposed higher demands than far-faults. The largest demand among all ground motions was caused by Yarimca record which produced the maximum link inelastic rotation of 0.23 and 0.28 rad, respectively for 12- and 15-story frames. Finally, from the average profiles it was observed that the links rotations of three sets of motions for these two high-rise frames, same as 4-story and 8-story frames, were in acceptable range and the links completely satisfy the requirement stated in FEMA 356 for LS performance level.

twelve story frame

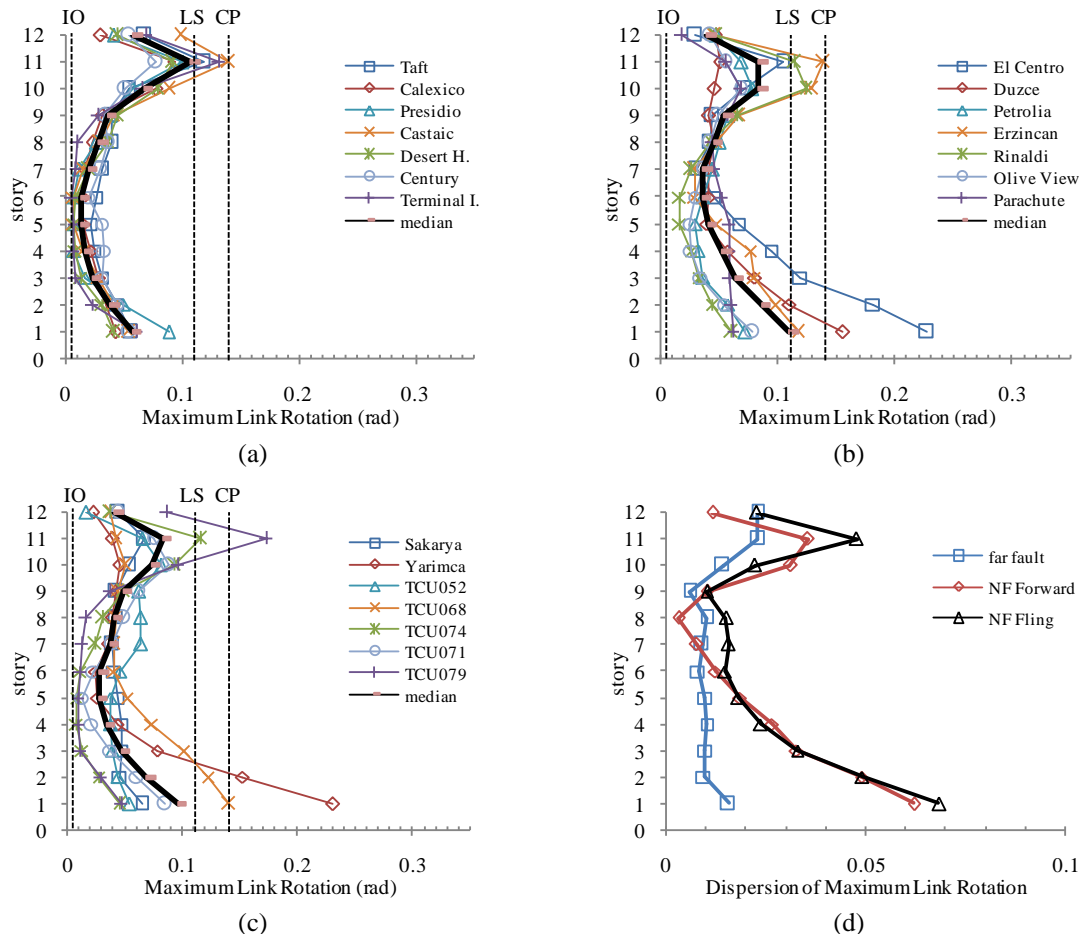


Fig. 7 Maximum link rotation of 12 story frame for (a) far-fault records, (b) near-fault records with forward directivity, (c) near-fault records with fling step, and (d) Dispersion of the results.

In EBFs after yielding of the links at upper and/or lower stories large plastic deformation occur in yielded elements while the other links remain in elastic range, i.e. EBFs are prone to develop soft-story mechanisms. This problem is distinguished in high-rise frames subjected to far-fault records and the deformations of many links in the middle portion of the frames are less significant. This confirms the nonuniform participation of links in energy dissipation. In case of near-fault records, although similar results observed, due to more effects of higher modes the demands in the middle stories are somewhat higher.

In Fig. 9, the severity of near-source records with forward-directivity and fling effects are compared with ordinary far-fault motions at the component level. The results shown are for a link on the first story level of the 4 story frame in which the maximum demand for each set of ground motions was caused by Taft, Rinaldi and TCU068 records. Although the results presented were for a typical link, but they convey the general difference in component demands between far- and near-fault earthquakes. In this figure, the normalized link shear forces obtained by dividing the

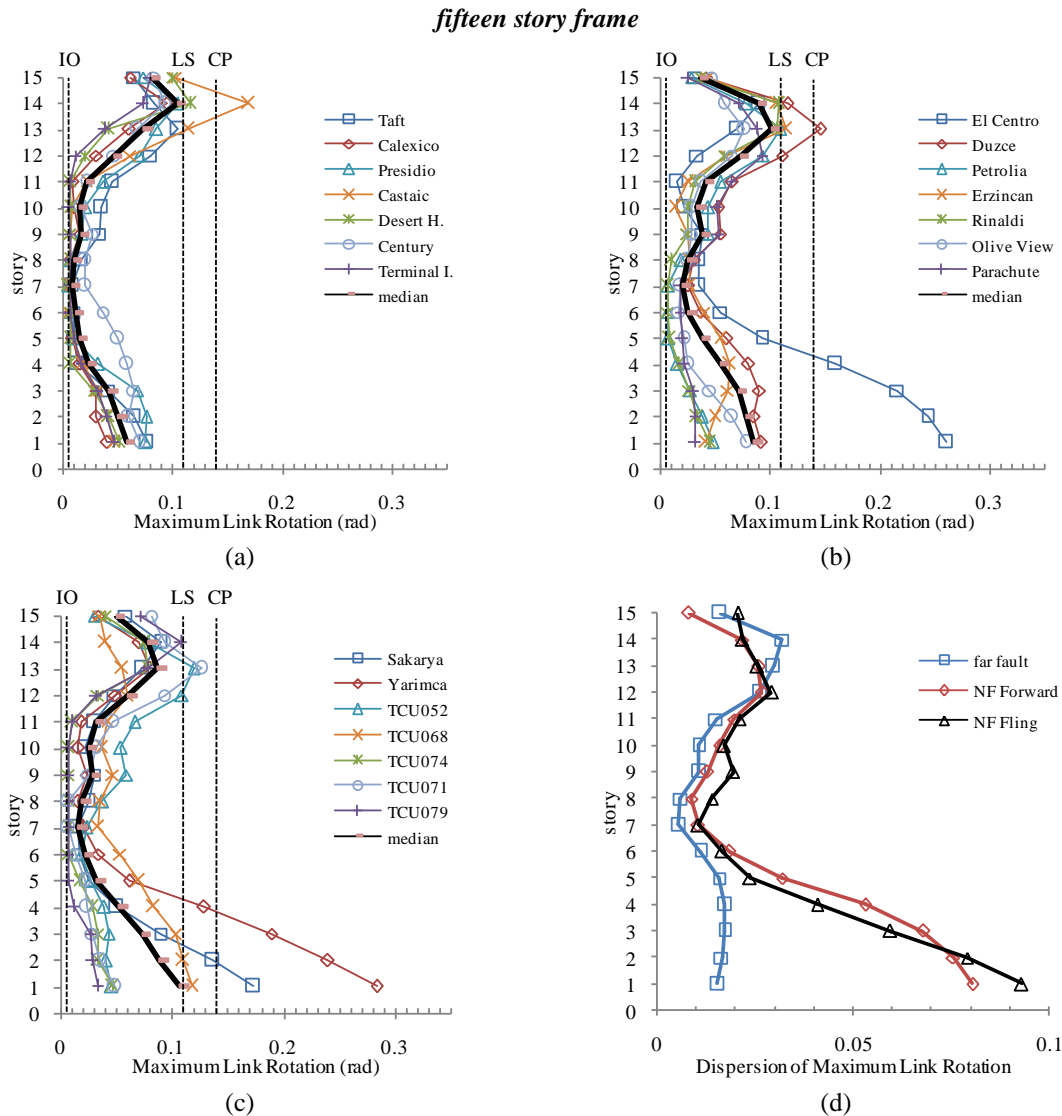


Fig. 8 Maximum link rotation of 15 story frame for (a) far-fault records, (b) near-fault records with forward directivity, (c) near-fault records with fling step, and (d) Dispersion of the results.

maximum link shear force values by the probable shear strength of the links ($1.1V_p$).

In EBFs, links web fracture before achieving their required rotation levels is the most common failure mode, which related to low cycle fatigue effects (Okazaki and Engelhardt 2007). For buildings subjected to Taft record (an ordinary far-fault record) many reversed cycles observe in hysteresis curve of link. These applied cycles in a cumulative manner may lead to web fracture and increase fatigue damage. On the other hand, near-fault motions are characterized by fewer inelastic deformation cycles among several elastic ones. For these records, due to arrival of the long-duration high-amplitude velocity pulses considerable energy is dissipated in limited inelastic deformations in a short period of time. Although the links under these ground motions experience

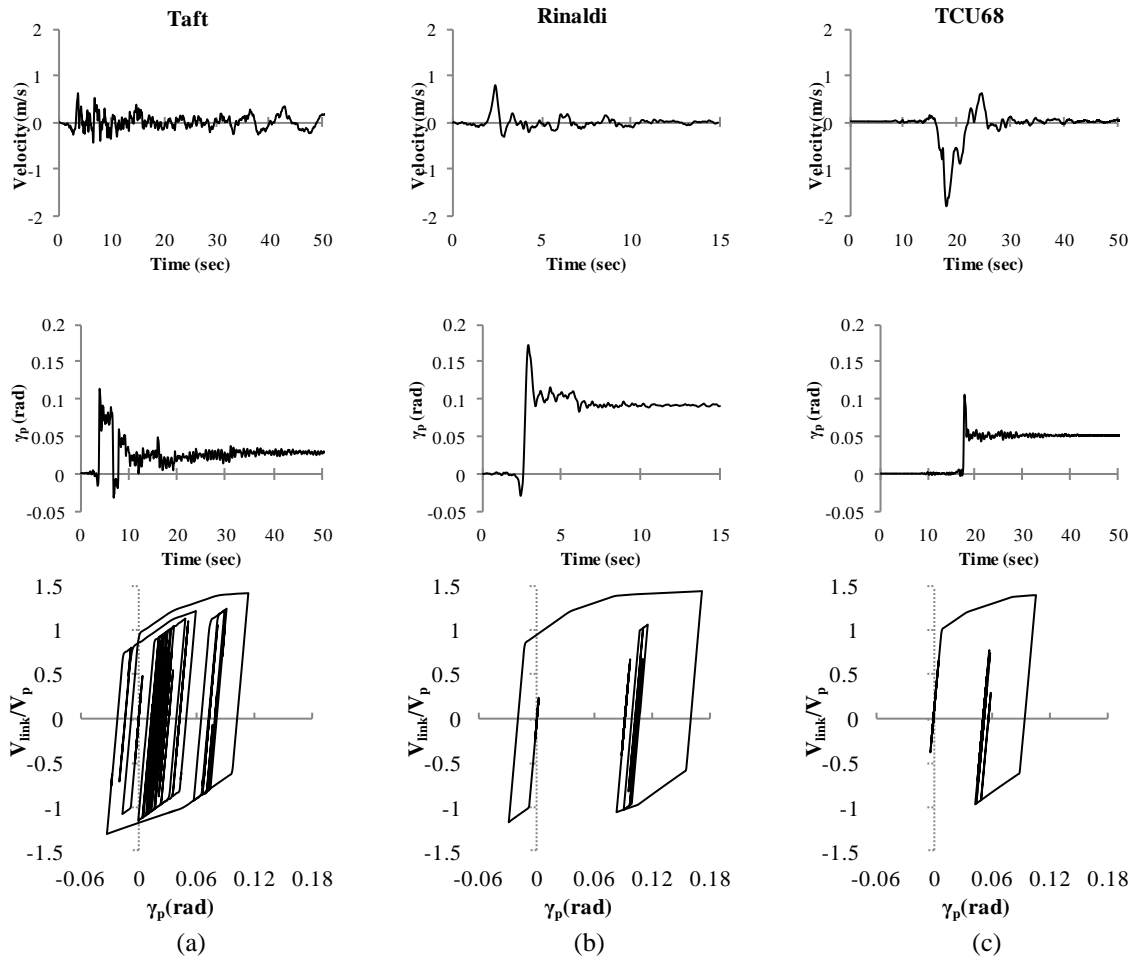


Fig. 9 Hysteretic behavior of a typical shear-link under (a) far-fault record (Taft), (b) near-fault record with forward-directivity (Rinaldi), and (c) near-fault record with fling-step (TCU68).

very large rotations, but effects of low-cycle fatigue for these links is less significant and they are capable of developing more values of inelastic rotation without strength degradation, on the basis of findings in (Okazaki and Engelhardt 2007).

6. Conclusions

In this study, consequences of well-known characteristics of near-fault earthquakes (forward-directivity and fling-step effects) on eccentrically braced buildings are assessed and the results are compared with typical far-fault records. The following conclusions can be made on the basis of the results of the study:

1. The median maximum links rotation of the frames subjected to three set of ground motions were in acceptable range and the links completely satisfied the requirement stated in FEMA 356

for LS performance level.

2. Eccentrically braced frames are prone to develop soft-story mechanisms. After yielding of the links at a story large plastic deformation occur in yielded element while the deformation of the other links is less significant.

3. For the 4 story frame, due to more effects of the first mode the maximum link rotation was concentrated at the first story for most records. For the other frames, depends on the frequency content of the motions the maximum demand was shown to be either at the upper or lower floors.

4. The minimum response of all frames was observed at the intermediate story levels. For high-rise frames under far-fault records many links in the middle portion of the frames was remained elastic, which confirms the nonuniform participation of links in energy dissipation. In case of near-fault records, though similar results were observed, due to more effects of higher modes the demands in the middle stories were somewhat higher.

5. Near-fault earthquakes in some cases were more destructive. Of the entire data set, for all frames the maximum link rotation was occurred by a fling-step record, with the exception of 4-story frame which forward-directivity records resulted in more demands.

6. The results of near-fault motions, especially records having fling effects, were so dispersed. Thus selection of more near-fault records produces more reliable results.

7. Many reversed cycles in hysteresis curve of links under a far-fault record increase low-cycle fatigue damage and may lead to web fracture before achieving links required rotation level, whereas effects of low-cycle fatigue for links under near-fault records is less significant and they are capable of developing more values of inelastic rotation without strength degradation.

Finally it is clear that the EBFs are suitable to use in near-fault regions with motions characterized by forward-directivity or fling effects. However, to gain further information about the performance of EBFs, this research should be continued by considering other characteristics of near-fault earthquakes and different bracing configuration.

References

- AISC (2005), *Seismic Provisions for Structural Steel Buildings*.
- AISC (2005), *Specification for Structural Steel Buildings*.
- Alavi, B. and Krawinkler, H. (2004), "Strengthening of moment-resisting frame structures against near-fault ground motion effects", *Earthq. Eng. Struct. Dyn.*, **33**(6), 707-722.
- American Society of Civil Engineers (2010), *Minimum Design Loads for Buildings and Other Structures*. ASCE/SEI 7-10.
- Champion, C. and Liel, A. (2012), "The effect of near-fault directivity on building seismic collapse risk", *Earthq. Eng. Struct. Dyn.*, **41**(10), 1391-1409.
- Chao, S.H. and Goel, S. (2005), "Performance-based seismic design of eccentrically braced frames using target drift and yield mechanism as performance criteria", Report UMCEE-05-05, University of Michigan, Ann Arbor, Mich.
- Charney, F. (2008), "Unintended consequences of modeling damping in Structures", *J. Struct. Eng.*, **134**(4), 581-592.
- Daneshmand, A. and Hosseini Hashemi, B. (2012), "Performance of intermediate and long links in eccentrically braced frames", *J. Constr. Steel Res.*, **70**(0), 167-176.
- Dicleli, M. and Mehta, A. (2007), "Effect of near-fault ground motion and damper characteristics on the seismic performance of chevron braced steel frames", *Earthq. Eng. Struct. Dyn.*, **36**(7), 927-948.
- Engelhardt, M.D. and Popov, E.P. (1989), "On design of eccentrically braced frames", *Earthq. Spectra*, **5**(3), 495-511.

- Gerami, M. and Abdollahzadeh, D. (2015), "Vulnerability of steel moment-resisting frames under effects of forward directivity", *Struct. Des. Tall Spec. Build.*, **24**(2), 97-122.
- Gerami, M. and Sivandi-Pour, A. (2014), "Performance-based seismic rehabilitation of existing steel eccentric braced buildings in near fault ground motions", *Struct. Des. Tall Spec. Build.*, **23**(12), 881-896.
- Ghobarah, A. and Ramadan, T. (1991), "Seismic analysis of links of various lengths in eccentrically braced frames", *Can. J. Civil Eng.*, **18**(1), 140-148.
- Ghodrati Amiri, G., Razeghi, H. and Tajik Davoudi, A. (2011), "The effect of fling step and forward directivity on the seismic response of MSSS bridges", *Tran. Res. J.*, **1**(1), 9-21.
- Hamidi Jamnani, H., Karbassi, A. and Lestuzzi, P. (2013), "Fling-step effect on the seismic behavior of high-rise RC buildings during the Christchurch earthquake", *2013 NZSEE Conference*, Wellington, New Zealand.
- Huang, L., Tan, H. and Yan, L. (2014), "Seismic behavior of chevron braced reinforced concrete spatial frame", *Mater. Struct.*, **48**(12), 4005-4018.
- Iervolino, I. and Cornell, C.A. (2008), "Probability of occurrence of velocity pulses in near-source ground motions", *Bull. Seismol. Soc. Am.*, **98**(5), 2262-2277.
- Kalkan, E. and Kunnath, S.K. (2006), "Effects of fling step and forward directivity on seismic response of buildings", *Earthq. Spectra*, **22**(2), 367-390.
- Kasai, K. and Popov, E. (1986), "General behavior of WF steel shear link beams", *J. Struct. Eng.*, **112**(2), 362-382.
- Koboevic, S. and David, S.O. (2010), "Design and seismic behaviour of taller eccentrically braced frames", *Can. J. Civil Eng.*, **37**(2), 195-208.
- Kuşyılmaz, A. and Topkaya, C. (2013), "Design overstrength of steel eccentrically braced frames", *Int. J. Steel Struct.*, **13**(3), 529-545.
- Kuşyılmaz, A. and Topkaya, C. (2015), "Fundamental periods of steel eccentrically braced frames", *Struct. Des. Tall Spec. Build.*, **24**(2), 123-140.
- Malhotra, P.K. (1999), "Response of buildings to near-field pulse-like ground motions", *Earthq. Eng. Struct. Dyn.*, **28**(11), 1309-1326.
- Mazzoni, S., McKenna, F., Scott, M. and Fenves, G. (2007), "OpenSees Command Language Manual".
- Menegotto, M. and Pinto, P. (1973), "Method of analysis for cyclically loaded reinforced concrete plane frames including changes in geometry and non-elastic behavior of elements under combined normal force and bending", *Proceedings of the LABSE, symposium on resistance and ultimate deformability of structures acted on by well defined repeated loads*.
- Mortezaei, A., Ronagh, H.R. and Kheyroddin, A. (2010), "Seismic evaluation of FRP strengthened RC buildings subjected to near-fault ground motions having fling step", *Compos. Struct.*, **92**(5), 1200-1211.
- Okazaki, T., Engelhardt, M., Nakashima, M. and Suita, K. (2006), "Experimental performance of link-to-column connections in eccentrically braced frames", *J. Struct. Eng.*, **132**(8), 1201-1211.
- Okazaki, T. and Engelhardt, M.D. (2007), "Cyclic loading behavior of EBF links constructed of ASTM A992 steel", *J. Constr. Steel Res.*, **63**(6), 751-765.
- Okazaki, T., Engelhardt, M.D., Drolias, A., Schell, E., Hong, J.K. and Uang, C.M. (2009), "Experimental investigation of link-to-column connections in eccentrically braced frames", *J. Constr. Steel Res.*, **65**(7), 1401-1412.
- Özhenekci, D. and Özhenekci, N. (2008), "Effects of the frame geometry on the weight and inelastic behaviour of eccentrically braced chevron steel frames", *J. Constr. Steel Res.*, **64**(3), 326-343.
- Popov, E.P., Ricles, J.M. and Kasai, K. (1992), "Methodology for optimum EBF link design", *Proceedings of the Earthquake Engineering, Tenth World Conference*, Balkema, Rotterdam.
- Richards, P. and Uang, C. (2005), "Effect of flange width-thickness ratio on eccentrically braced frames link cyclic rotation capacity", *J. Struct. Eng.*, **131**(10), 1546-1552.
- Richards, P. and Uang, C. (2006), "Testing protocol for short links in eccentrically braced frames", *J. Struct. Eng.*, **132**(8), 1183-1191.
- Rides, J. and Popov, E. (1994), "Inelastic link element for EBF seismic analysis", *J. Struct. Eng.*, **120**(2), 441-463.

- Soleimani Amiri, F., Ghodrati Amiri, G. and Razeghi, H. (2013), "Estimation of seismic demands of steel frames subjected to near-fault earthquakes having forward directivity and comparing with pushover analysis results", *Struct. Des. Tall Spec. Build.*, **22**(13), 975-988.
- Somerville, P. (1998), "Development of an improved representation of near-fault ground motions", *Proceedings, Seminar on Utilization of Strong-Motion Data*, Oakland, CA.
- Tsai, K.C., Yang, Y.F. and Lin, J.L. (1993), "Seismic eccentrically braced frames", *Struct. Des. Tall Spec. Build.*, **2**(1), 53-74.
- Uriz, P., Filippou, F. and Mahin, S. (2008), "Model for cyclic inelastic buckling of steel braces", *J. Struct. Eng.*, **134**(4), 619-628.
- Vafaei, D. and Eskandari, R. (2015a), "Seismic performance of steel mega braced frames equipped with shape-memory alloy braces under near-fault earthquakes", *Struct. Des. Tall Spec. Build.*, doi: 10.1002/tal.1225.
- Vafaei, D. and Eskandari, R. (2015b), "Seismic response of mega buckling-restrained braces subjected to fling-step and forward-directivity near-fault ground motions", *Struct. Des. Tall Spec. Build.*, **24**(9), 672-686.
- Viswanath, K.G., Prakash, K.B. and Desai, A. (2010), "Seismic analysis of steel braced reinforced concrete frames", *Int. J. Civil Struct. Eng.*, **1**(1), 114-122.